České vysoké učení technické v Praze, Fakulta stavební

Czech Technical University in Prague, Faculty of Civil Engineering

Ing. Bohumil Kasal, PhD, MS, MS

Professor of Civil and Environmental Engineering, Professor of Architectural Engineering, Hankin Chair of Residential Building Construction, Penn State University

Local Reinforcement of Wood with Composite Materials

Summary

Applications of composite reinforcement to wood structural members and connections are discussed. The paper focuses on local reinforcement that mitigates brittle failures due to tension perpendicular to wood fibers. The effectiveness of radial reinforcement is demonstrated via experiments and analysis. In order for composite reinforcement to be applicable in a design practice, a number of questions related to long-term performance, durability and fire resistance must be answered. These include: compatibility between reinforcing and reinforced materials due to thermo-expansion and differential shrinkage and swelling, creep and mechano-sorptive creep behavior, behavior of the adhesive interface under elevated temperatures and aggressive environments. Two examples of the application of composite materials in timber structures are discussed: radial reinforcement of laminated arches and perpendicular-to-fibers reinforcement of beam-to-column connections. Reinforcement of arches is facilitated via glass-fiber rods and pre- and post-crack behaviors are analytically studied.

The radial reinforcement of beam-to-column connections of frames (moment connections) is demonstrated via small- and full-scale experiments. Radial reinforcement fully mitigates brittle connection failures and significantly enhances moment capacity and ductility of the connection. Energy dissipation mechanisms are indentified as friction, steel dowel yielding and wood crushing. An analytical model is proposed to model each of the individual phenomena. The model is phenomenological but its parameters are related to physical properties of connected components. A system of springs, sliders and gaps is used to model overall hysteretic connection behavior. A parameter extraction process has been proposed and validated via experiments and evaluation of the dissipated energy. In the second experiment, an arbitrary load was used to generate a hysteretic response and the experiments were compared with the analytical model subjected to an identical load history. Energies per cycle, cumulative dissipated energies and moment-rotation curves were compared. The model replicated the experimental moment-rotation relationship reasonably well. While the global (cumulative dissipated energy) criterion was satisfactory, the error in dissipated energy per individual load cycle can be relatively large.

Souhrn

Přednáška se zabývá lokálním vyztužením prvků dřevěných konstrukcí za účelem zamezení křehkého lomu v důsledku tahového namáhání ve směru kolmo k vláknům. Efektivnost radiálního vyztužení je demonstrována pomocí experimentů a analyticky. Před tím, než lze vyztužení kompozitními materiály aplikovat v praxi, je třeba zodpovědět řadu otázek týkajících se dlouhodobého působení, životnosti a protipožární odolnosti. Další parametry, které je nutno studovat, zahrnují kompaktibilitu mezi vyztužujícím a vyztužovaným materiálem vlivem diferenciální tepelné a vlhkostní roztažnosti, tečení a mechanosorbční tečení, jakož i chování mezní vrstvy za zvýšených teplot a chování v agresivním prostředí. Použití kompozitních materiálů v dřevěných konstrukcích je demonstrováno na příkladech lepeného lamelovaného oblouku a momentového spoje rámové konstrukce. Vyztužení oblouku je realizováno pomocí vlepených sklolaminátových tyčí a chování systému před a po vzniku trhlin je experimentálně a analyticky vyhodnoceno. Radiální vyztužení rohových rámových spojů je provedeno pomocí sklolaminátové kompozitní textilie s epoxidovou matricí a je experimentálně demonstrováno. Radiální vyztužení plně odstraňuje křehká porušení a významně zvyšuje kapacitu a schopnost spoje pohlcovat energii. Mechanismy, které kontrolují pohltivost energie, jsou identifikovány jako tření a plastické deformace oceli a dřeva v oblasti kontaktu. Pro každý mechanismus je navržen analytický model, který sestává ze systému pružin, mezer a třecích prvků. Model je sice fenomenologický, ale individuální parametry reprezentují fyzikální vlastnosti spoje. Systém pružin, mezer a třecích prvků kombinovaných v sérii a paralelně je použit na modelování hystereze. Identifikace parametrů modelu je ověřena pomocí experimentů a vyhodnocením pohlcené energie. Náhodné cyklické zatížení je použito na vyhodnocení obdržených parametrů modelu a experiment je porovnán s modelem, který je zatížen stejnou historií. Na vyhodnocení kvality modelu je použita energie na cyklus, kumulativní pohlcená energie a křivky zobrazující vztah mezi momentem a rotací. Model reprezentuje experimentální data poměrně dobře pro kumulativní hodnoty pohlcené energie, avšak chyba v energii na jeden cyklus může být značná.

Klíčová slova: dřevo, vyztužení, kompozitní materiály, nelineární chování, hystereze, pohlcení energie, model

Keywords: wood, reinforcement, composite materials, nonlinear behavior, hysteretic behavior, energy dissipation, model

—

České vysoké učení technické v Praze
Název: Lokální vyztužení dřeva kompozitními materiály

Autor: Ing. Bohumil Kasal, PhD, MS, MS, Professor of Civil and Environmental Engineering, Professor of Architectural Engineering, Hankin Chair of Residential Building Construction, Penn State University

Počet stran:
Náklad:

Contents

1 INTRODUCTION 6
2 RADIAL REINFORCEMENT OF CURVED BEAMS AND ARCHES 7
3 RADIAL REINFORCEMENT OF MOMENT CONNECTIONS 11
3.1 MODEL OF THE NONLINEAR, NONCONSERVATIVE SPRING ELEMENT 14
3.2 PARAMETER IDENTIFICATION 15
3.3 PARAMETER EVALUATION 18
3.4 VALIDATION OF THE CONNECTION MODEL 20
4 CONCLUSIONS 25
5 ACKNOWLEDGMENT 25
6 LITERATURE CITED 26
CURRICULUM VITAE 29

1 INTRODUCTION

In the past decade, wood has experienced a renaissance as a structural material of choice due to its aesthetic and environmental properties. Glue-laminated wood technology (glulam) was developed at the beginning of the last century and evolved rapidly with the advent of synthetic adhesives such as phenol-resorcinol or polyisourethanes. A high strength/weight ratio significantly exceeding the ones of concrete or steel and their high fire resistance make glulam beams ideal for large-span structures. In addition, natural resistance of wood to aggressive environments such as a corrosive atmosphere or exposure to salts are attributes increasing efficiency and environmental friendliness of the material. Examples of large-span structures exceeding a free span of 50 m are numerous [2]. Wood, however, possesses some drawbacks such as hygroscopicity, susceptibility to biotic attack if not protected from moisture, anisotropic characteristics and high variability of properties. In this paper, the anisotropic character and mitigation of its implications will be discussed.

Wood has high tensile and compressive strength in the direction along fibers and low tensile strength across fibers. This makes is difficult to use wood in structural components where radial stress (tensile stress across fiber) is inevitable. This includes arches, non-prismatic beams and moment connections. While some national and international standards [3, 4, 5] permit minimum design stress in radial tension, it is a serious limitation. Likewise, moment connections are subjected to radial tension that results in a brittle type of failure, which may be extremely dangerous in seismic zones. Radial reinforcement of wood in the direction across fibers has been used as a mean of increasing tensile strength perpendicular to fibers and shifting failure modes from brittle to ductile. In most cases, composite fabric of various designs was used as a reinforcing medium. The fabric was attached to the surface of members and prevented crack formation and development, at least in zones reasonably close to the surface [5]. Another reinforcement strategy is using glued-in composite fiber rods in a radial direction. In both cases, the interface between reinforced and reinforcing material must transfer strains during pre- and post-crack

phases of deformation. Some issues that must be resolved for the reinforcement to function properly are:

- Compatibility in strains
- Compatibility in shrinkage and swelling
- Compatibility in thermo expansion properties
- Time- and load-history dependent properties of the adhesive layer and the composite system

The ultimate strain in tension perpendicular to fibers are important factors in determining properties of reinforcing material, which must be able to transfer significant loads after cracks between fibers develop. The shrinkage and swelling and thermo expansion compatibilities must be maintained to prevent the development of interfacial stresses due to differential shrinkage/swelling or thermal expansion. The long-term behavior of the interface between reinforced and reinforcing materials is of particular importance when combined with sorption/desorption associated with the hygroscopic nature of the material. The mechanosorptive creep must be studied to avoid potential interface failures and/or delaminating.

2 RADIAL REINFORCEMENT OF CURVED BEAMS AND ARCHES

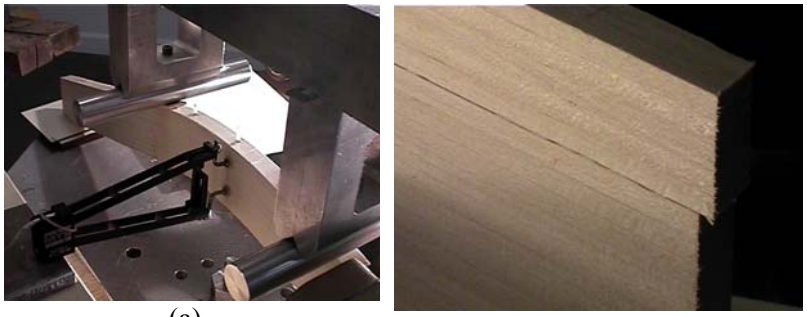

(a) (b)

Figure 1. Bending test of curved beam with radial reinforcement [1]. (a) Test setup, and (b) failure of an unreinforced beam due to the radial crack propagation.

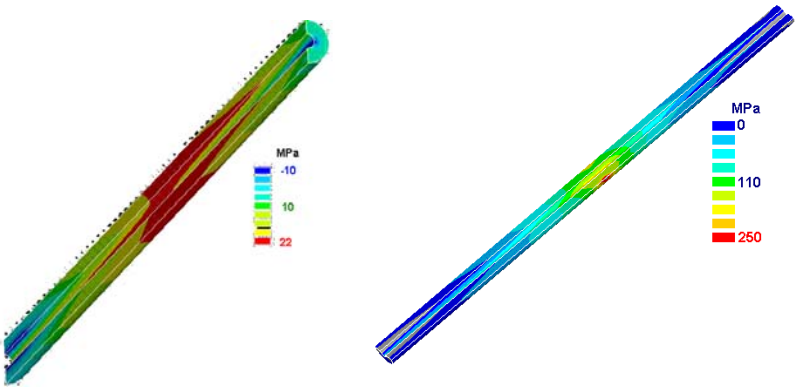

(a) (b)

Figure 2. Pre- (a) and post-crack (b) stress in the glass-fiber reinforcing rod.

The first example involves radial reinforcement of a glue-laminated curved beam. Curved beams are common in wood structures due to the convenient stress distribution that tends to be compressive. The negative consequence of the curvature, however, is the development of radial tensile stresses in the curved part of the beam. The strength of wood in radial tension (or tension perpendicular to fibers) is very low compared to stresses along the fibers with a yield strain of about 0.1% [1]. This creates a situation where radial stress can create cracks in the zones with a maximum bending moment, which can then propagate along the beam. A model of a laminated, curved beam was constructed and glass fiber rods were glued in the radial direction as shown in Figure 1. The geometry of the beam was designed such that radial stress would produce cracks at the beam's crest. A surface strain was observed with digital image processing and from an extensometer mounted at the location with expected extreme stress. Elastic constants including a tensile stress-strain relationship for the perpendicular-to-fibers direction were experimentally measured to suppress contamination of the analysis by data variability. Figure 2 shows the values of stress in the reinforcing rod before and after crack development. The increase in stress is significant and shows the effectiveness of the reinforcement. This is a numerically calculated value since rods were not instrumented during the experiments.

The value of the verified analytical model is in its ability to simulate various parameters that will require involved testing procedures. The parameters of interest may include: reinforcing rod properties (such as stiffness, diameter, and spacing), beam geometry and properties and various loading and boundary conditions. The GF rods can be used in the repair of laminated beams failing in radial tension. The tests and an analysis of post-crack behavior showed that the reinforcement was capable of arresting the cracks and transferring the load through the interface.

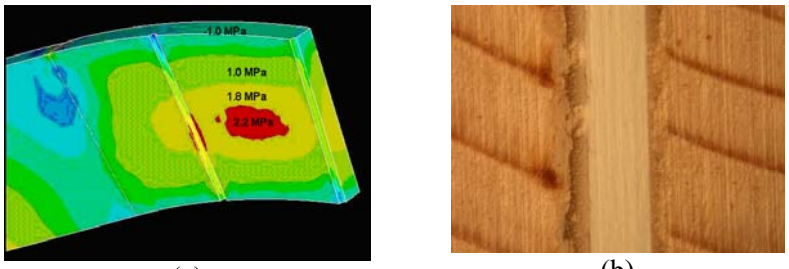

(a) (b)

Figure 3. Stress distribution in a reinforced, curved beam (a), and (b) the interface between GF reinforcement and wood (40 x).

Figure 3a shows the theoretical stress distribution in a reinforced, curved beam. Failure in radial tension (2.2 MPa) is expected in zones between reinforcement and even at the interface between the rod and wood. This confirms the experimental observation where cracks developed in the reinforced and unreinforced beams. The difference is in the capability of the reinforcement to arrest the cracks. Figure 3b shows the microscopic image of GF reinforcement bonded with epoxy resin to wood material. The dark, horizontal lines represent late wood; the epoxy layer is clearly visible. The interface needs to be carefully studied since interfacial stresses can result in shear failure of the bond. Figure 4 shows a radiographic image of an internal reinforcement of laminated arch. The real-time, digital radiography can be used to evaluate internal crack development. The system resolution is currently limited but offers opportunities to measure internal deformations of the reinforcing systems.

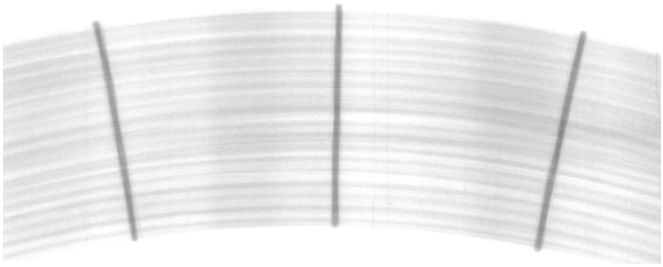

Figure 4. Radiographic image of glass-fiber radial reinforcement of an arch.

Compatibility between reinforcing and reinforced materials is important in minimizing residual stresses due to differential shrinkage and swelling and different thermo expansion coefficients. Composite pipes permit designing the reinforcement with a desired stiffness and strength. Variables that can be controlled include wall thickness of the composite pipe, pipe diameter, type of longitudinal and transverse fibers, angle of transverse reinforcement, and matrix type - Figure 5.

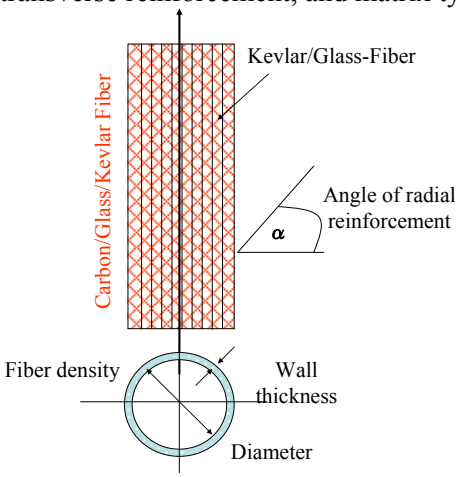

Figure 5. Geometry of reinforcing composite pipe and variables affecting the performance of the reinforcement.

3 RADIAL REINFORCEMENT OF MOMENT CONNECTIONS

The second example involves beam-to-column moment connections of laminated timber frames. The moment connections of wood structures always include mechanical fasteners that are usually in the form of steel dowels, pins or bolts. Transferring moments and normal forces result in a tension perpendicular to fibers and subsequent potential brittle failure. A body of knowledge exists about the application of surface reinforcement using composite fabric such as glass-fiber nonwoven material with epoxy matrix. The problem with using surface application is that it is effective only in close vicinity of application and cracks can develop far from the restrained surface (Saint-Venant's principle applies here). Using composite rods alleviates this problem. Figure 6 shows the effect of reinforcement on the failure mode of a moment connection.

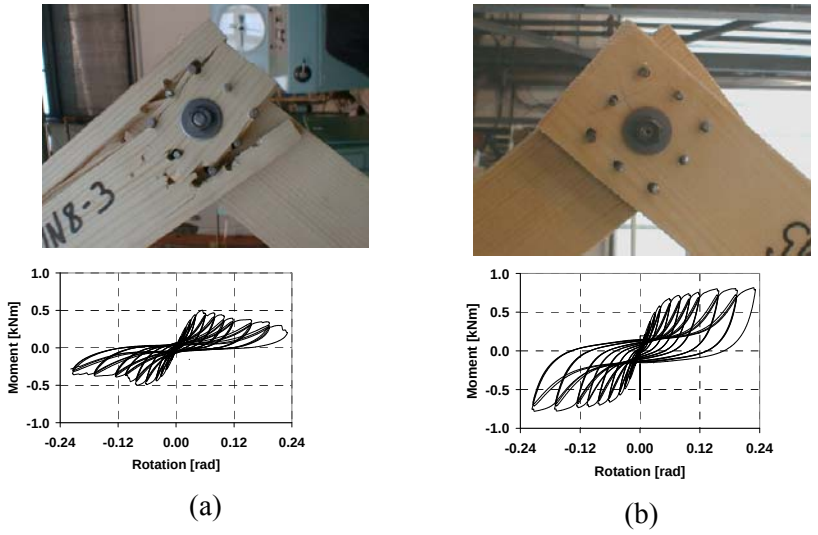

(a) (b)

Figure 6. Beam-to-column connections subjected approximately to the same rotations (a) unreinforced and (b) reinforced.

The connection in Figure 6a failed in brittle manner while the connection in Figure 6b showed no sign of cracks and failure under large rotations. Such behavior is important especially in dynamically

loaded structures where brittle failure is not acceptable. The moment-rotation curves shown in Figure 6 clearly demonstrate the effect of radial reinforcement on moment capacity of the beam-to-column connections. One of the measures of the effectiveness of moment connections is their capability to dissipate energy. Relatively large rotations are required to take the advantage of the dissipative capacity of the reinforced systems. The dissipative capacity of a reinforced connection is demonstrated in Figure 7. The GF reinforced connection dissipated significantly more energy without crack developments or failure. Large rotations will result in large drifts of composite reinforced frames without failures.

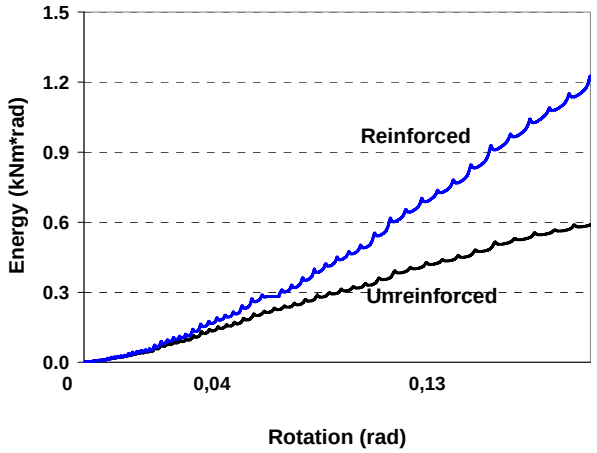

Figure 7. Energy dissipation of a cyclically loaded beam to column connection.

The internal deformation of the dowel-type connection is shown in Figure 8. The reinforcement permits designing a balanced connection in which the steel and connected materials yield at roughly equivalent moments thus increasing the energy dissipation capacity of the reinforced system.

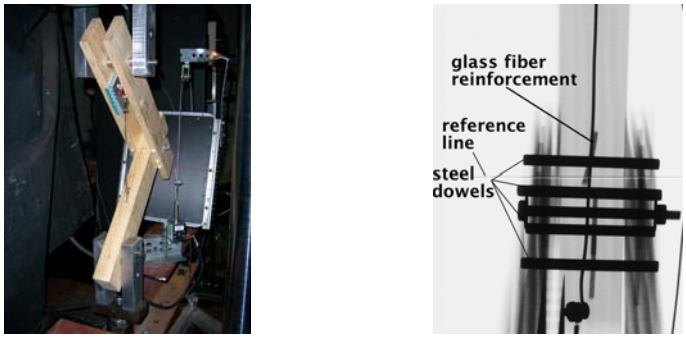

(a) (b)

Figure 8. Test of reinforced beam-to-column connection: (a) test setup and (b) X-ray image.

The radiographic image quantitative analysis was applied to extract the strains of cyclically loaded moment connections – Figure 9. Simple moment-curvature analysis can be used to extract strains in the steel pins. The information can be used to verify design assumptions such as yield theory that is frequently used in connection design [9].

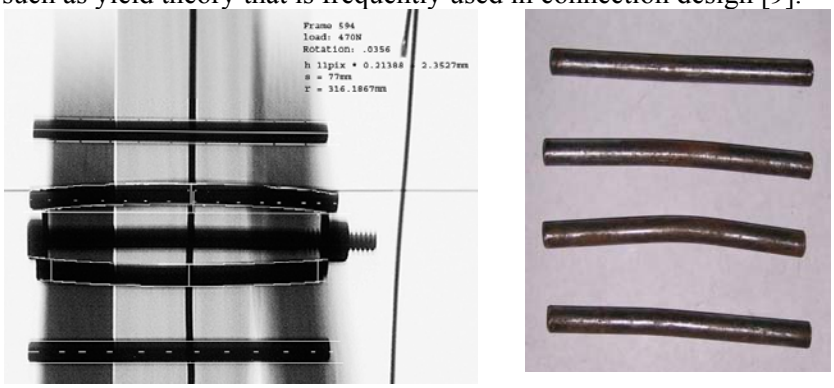

(a) (b)

Figure 9. Radiographic image of cyclically loaded beam-to-column connection (a) and corresponding dowel deformation (b).

ANALYTICAL MODELS OF CONNECTIONS

Modeling the beam-to-column connections in analytical models of frames requires nonlinear analysis due to the non-conservative

connection behavior. Achieving accurate results in a nonlinear time-history analysis requires accurate hysteretic connection models since the joints are responsible for most of the damping of inelastic systems [25]. Many hysteresis models have been proposed to describe the load-history dependent behavior of timber joints subjected to cyclic loads [14, 15, 16]. Well known is the DRAIN 2DX program from Powel [17] for the dynamic analysis of nonlinear structures. Kasal et al [18, 19] and Collins et al [20] developed a special hysteretic finite-element with strength and stiffness degradation properties. This approach has been successfully used in light-frame and steel structures but requires attaching a specialized code to a generic finite-element package and recompiling the entire software [12]. Fajfar and Drobnic [22] and Pradhan [23] used a simple approach to simulate the nonlinear dynamic behavior of BC connections of reinforced concrete composites, where the hysteretic behavior of concrete was modeled using bilinear elasto-plastic springs with gaps. Kawai [24] used a similar approach to model the behavior of nailed shear walls used in wood frame constructions.

Most of the models mentioned above are phenomenological - they describe the nature of a load-deformation relationship based on experimental measurements but do not necessarily explain the mechanics of the joint itself [21]. The connection model proposed in this paper provides more insight into the response of the connection as affected by material properties and mechanics of the individual elements.

3.1 MODEL OF THE NONLINEAR, NONCONSERVATIVE SPRING ELEMENT

To capture the hysteretic, load-history dependent behavior of the connections between frame members a nonlinear, nonconservative spring element was generated. The connection behavior was modeled via a combination of linear spring-, slider- and gap-elements available within most structural analysis finite element packages [12]. The combination of spring-, slider- and gap-elements allows modeling of various hysteretic shapes including pinching, asymmetric behavior, contact phenomena, and initial slip of the fasteners. Modeling large initial slippage in the joints is a decisive advantage, which allows the simulation of an aftershock scenario. The model is not capable

capturing strength degradation and/or the brittle failure of the joint. Several elements are required to describe the connection behavior with sufficient accuracy.

3.2 PARAMETER IDENTIFICATION

Three modes of energy dissipation in the connections were considered using a system of nonlinear springs to represent the following behavior:

(I) Friction between beams and column
(II) Bending of the dowel-type fasteners
(III) Embedding behavior of wood

The load-deformation relationship is a summation of individual components. Since the spring elements are connected in parallel they can be studied separately based on the load-carrying behavior of the individual parts - see Figure 10.

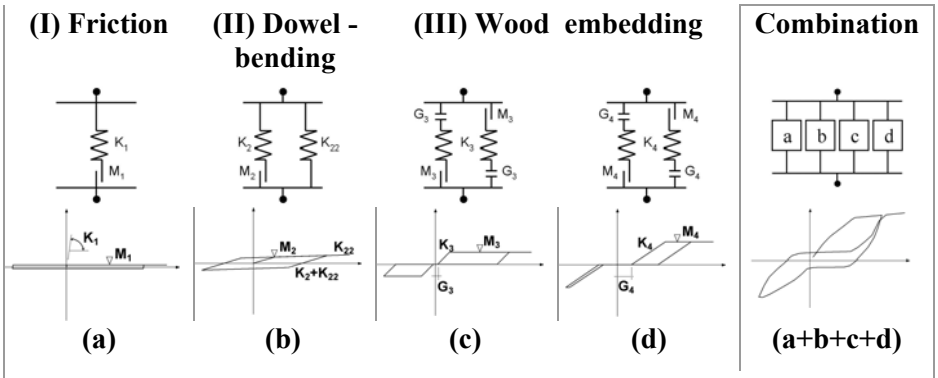

Figure 10. Connection model using combination of spring-, slider- and gap-elements

(I) Friction between beams and column

Figure 11 shows the hystereses of a small-scale connection subjected to a cyclic load procedure according to the DIN EN 12512 [25]. Two

experiments per connection were carried out. In the first test pure friction between beams and column was simulated by a center bolt pressing together the wood members (no drift-pins). The moment applied to tighten the nut of the center bolt M8 was 8.6 Nm. After finishing this test, the drift pins were driven into the predrilled holes and the test was repeated. Comparison of the moment-rotation curves proved that friction between the beams and column was constant and independent of the load-history. The results justify defining the frictional effect as a separate system, independent of the load-history.

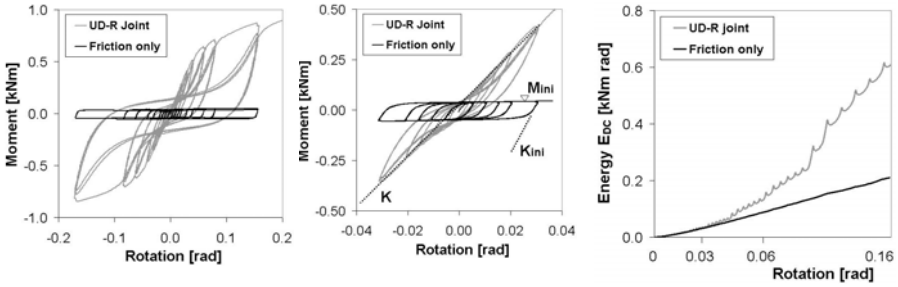

(a) **(b)** **(c)**

Figure 11. Comparison between a joint with and without fasteners (UD-R joint design)

Figure 11a shows the moment-rotation curves up to a rotation of 0.2 rad and Figure 11b shows the same hysteresis for small rotations less then 0.03 rad. It was observed that for such small amplitudes the degradation in strength was negligible. Consequently, the error due to degradation, not considered in the analytical model, will be small at this rotation level. The frame experiments reported in [26] showed that the beam-to-column connections in the two-story laminated frames rotated about 0.012 to 0.023 rad at extreme story drifts. Such small amplitudes resulted in negligible strength degradation. The initial stiffness K_{ini} due to the friction was about 39 kNm/rad, whereas the stiffness K of the connection was about 14 kNm/rad. The maximum moment M_{ini} reached during the friction test was constant 0.04 kNm.

Figure 11c shows that up to a joint rotation of 0.03 rad the energy dissipated from the connection was almost entirely due to the frictional effects, while for larger joint rotations most of the energy gets dissipated through the plastic deformation of wood and steel fasteners.
A bilinear spring element with a rotational stiffness K_1 [kNm/rad] and a sliding moment M_1 [kNm] was used to simulate the friction of the connections (Figure 10a). The model represents the cyclic behavior of elastic -plastic material with non-conservative unloading.

(II) Bending of the dowel-type fasteners

The characteristics of the steel fasteners were represented by a combination of a bilinear, elastic-plastic spring (K_2 and M_2) and a linear spring K_{22} connected in parallel (Figure 10b). The beginning of the plasticization is defined by the sliding moment M_2. The presence of K_{22} increases the stiffness, but does not result in a change of energy dissipation [12].

(III) Embedding behavior of wood

In order to approximate the load-history dependent connection behavior, a spring element with memory was defined. The modeling of the unrecoverable plastic deformation of wood was done by spring (K_3, K_4), slider (M_3, M_4) and gap elements (G_3, G_4) connected in series (Figure 10c and d). Therefore, two elements were necessary: one for tension (1st quadrant) and one for compression (3rd quadrant). The use of gaps allowed the simulation of the initial slip due to fabrication tolerances and/or damage due to previous loading. To define the asymmetric hysteretic behavior, different values for K_j, M_j and G_j (1st and 3rd quadrant) must be used. To increase the accuracy of the model a larger number of bilinear spring elements is required.
The general function of the envelope curve $M(\varphi)$ in the 1st quadrant (Figure 12) is expressed with following equation:

$$M(\varphi) = \sum_{j=1}^{4} K_j \cdot \varphi_j + K_{22} \cdot \varphi \qquad \textbf{(1)}$$

if $\varphi \le G_j$ *then*

$\varphi_j = 0$

else

$\varphi_j = (\varphi - G_j)$

if $\varphi_j \ge \dfrac{M_j}{K_j}$ *then*

$\varphi_j = \dfrac{M_j}{K_j}$

where: K_j, M_j and G_j = constants of element j presented in Figure 10 ($G_1 = G_2 = 0$)

3.3 PARAMETER EVALUATION

To obtain model parameters from experimental data, a parameter search routine was developed. First the envelope curve of the analytical model, expressed by equation 1, should match the non-stabilized (1st cycle) envelope obtained in the cyclic test. If the connection exhibits significant strength and stiffness degradation, the stabilized 2nd cycle should be used. Figure 12 shows the location of characteristic points that were used to extract the parameters K_j, M_j and G_j from hysteresis.

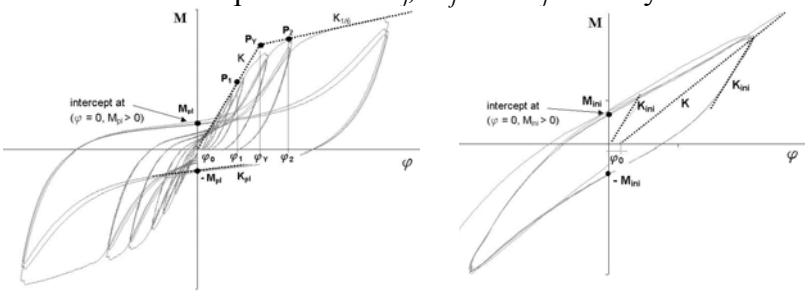

(a) **(b)**

Figure 12. Location of points for a symmetric hysteresis: (a) entire hysteresis and (b) hysteresis of the first cycle with an amplitude $\varphi = 0.25\ \varphi_y$

The yield point P_Y, the stiffness K and the stiffness $K_{1/6}$ are defined in the DIN EN 12512 [11]. Further constants are defined as follows:

M_{ini} = moment at the intercept of the first cycle with an amplitude φ = 0.25 φ_y
K_{ini} = initial slope of the first cycle (about equal to the slope of unloading function)
P_1 = point of first yielding
P_2 = point of first contact between the hysteresis and $K_{1/6}$ (plasticized joint)
K_{12} = slope defined by P_1 and P_2
M_{pl} = moment at the intercept of the cycle with an amplitude φ_{pl} = 3 φ_y
K_{pl} = slope of the descending curve at the intercept M_{pl}
φ_0 = initial slip - rotation at the intersection of K and the X-axis ($\varphi_0 \geq 0$)

The total number of parameters K_j, M_j and G_j that need to be extracted from cyclic experiments is eleven. They are evaluated in accordance to the following equations:

$$
\begin{aligned}
M_1 &= M_{ini} \\
K_1 &= K_{ini} \\
M_2 &= M_{pl} - M_{ini} \\
K_2 &= M_2 / \varphi_Y \\
K_{22} &= K_{pl} \\
G_3 &= \varphi_0 \\
K_3 &= K - (K_2 + K_{22}) \\
M_3 &= K_3 \cdot (\varphi_1 - \varphi_0) \\
G_4 &= \varphi_1 \\
K_4 &= K_{12} - K_{22} \\
M_4 &= K_4 \cdot (\varphi_2 - \varphi_1)
\end{aligned}
\qquad \textbf{(2)}
$$

This set of equations is used to determine the element parameters. A summary of the full-scale connection parameters used in time-history analysis is given in the Table 1.

Table 1. Parameters of the full-scale connections

Parameter	Unit	Source	Reference		Alternative	
			BC	CF	BC	CF
K_1	kNm/rad	Friction	3500(1)	3500(1)	3500(1)	3500(1)
M_1	kNm		1.2	0.8	1.4	1
K_2	kNm/rad	Dowel (bending)	140	2000	360	2500
M_2	kNm		4	5	7.6	10
K_{22}	kNm/rad		30	260	60	400
K_3	kNm/rad	Wood (embedding crushing)	500	1300	1000	1800
M_3	kNm		8	22	22	40
G_3	rad		0.003	0.0026	0.002	0.004
K_4	kNm/rad		330	1000	600	1500
M_4	kNm		12	40	19	38
G_4	rad		0.019	0.0195	0.022	0.026

(1) No test data were available to determine the initial stiffness K_{ini} of the full-scale connections. Therefore a value of 3500 kNm/rad had been chosen based on the initial slope at the first hysteretic loop. As long as the sliding moment M_1 is small, K_1 is of minor importance for the accuracy of the model. Small deviations in stiffness will have insignificant effects on the amount of dissipated energy.

3.4 VALIDATION OF THE CONNECTION MODEL

The accuracy of the connection model will be examined by comparing the predicted hysteretic responses against experimental data. Figure 13 shows the experimental versus analytical results for the full-scale connection.

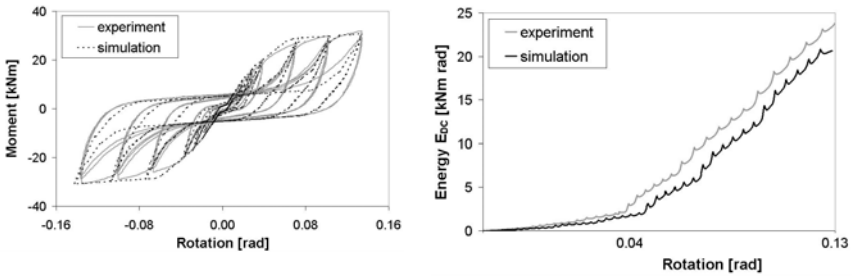

Figure 13. Simulation versus experimental results for the full-scale BC connection

The proposed model was capable of capturing the time-history response of the connection with sufficient accuracy. Accurate estimation of the entire load-deformation response is important as this affects not only maximum displacements but also the level of energy dissipation. Since energy dissipation accounts for most of the system damping correctly estimating this part of the hysteretic response is paramount. In the parameter identification above, the parameters were obtained without regard to the energy dissipated and thus may provide an incorrect system response. Thus energy dissipation may be used to evaluate the quality of the model obtained from the characteristic points defined earlier. Figure 13 and Table 2 compare the dissipated energy of the connection model with that of experimental data. The error listed in Table 2 is defined as the experimental result – analytical result / experimental result. The results show that the error of the simulation was kept at a reasonable level.

Table 2. Dissipated energy of the model compared with the experiment

Cycle number	Rotation [rad]	Cumulative Energy E_{DC} [kNm rad]		Error [%]
		Simulation	Experiment	
1	0.009	0.13	0.11	18
2	0.019	0.45	0.39	13
3	0.027	1.00	1.03	-3
4	0.036	2.06	2.20	-6
5	0.068	5.90	6.40	-8
6	0.101	12.4	13.8	-10
7	0.134	20.8	24.6	-15

Another useful quantitative method in demonstrating the validity of the hysteretic analytical model is to simulate the response of a system subjected to arbitrary loading. Such a loading sequence is presented in Figure 14a. This sequence reflects qualitatively the deformation history that full-scale connections sustained during a shake table experiment. The arbitrary loads were applied to a small-scale joint with the resulting load-deformation response shown in Figure 14b. The moment-rotation curve was used to extract the characteristic points as shown in Figure 12. The spring parameters of the model were then evaluated in accordance to equations 2. The resulting parameters are listed in Table 3.

Table 3. Characteristic values and spring parameters for a small-scale joint

Charact. values	K_{ini}	M_{ini}	K	M_{pl}	K_{pl}	φ_y	M_y	φ_0	φ_1	φ_2	K_{12}
	25	0.025	11	0.05	0.63	0.033	0.42	0.0005	0.022	0.062	3.6
Spring parm.	K_1	M_1	K_2	M_2	K_{22}	K_3	M_3	G_3	K_4	M_4	G_4
	25	0.025	0.76	0.025	0.63	9.61	0.21	0.0005	2.97	0.12	0.022

The analytical versus experimental results are shown in Figure 14b.

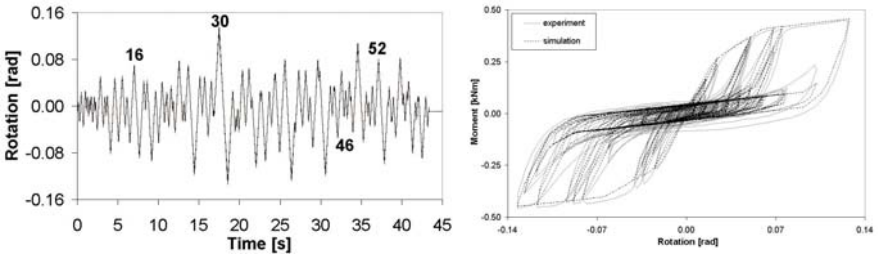

(a) **(b)**

Figure 14. (a) arbitrary-load procedure and (b) moment-rotation curves of simulation versus experiment

Figure 14 shows that the prediction over the entire load-history is qualitatively in good agreement with the experimental results. In Figure 15 selected cycles were plotted to see more clearly the ability of the model to capture the hysteretic response. The selected cycles are labeled in rotation time-history inset of Figure 14a.

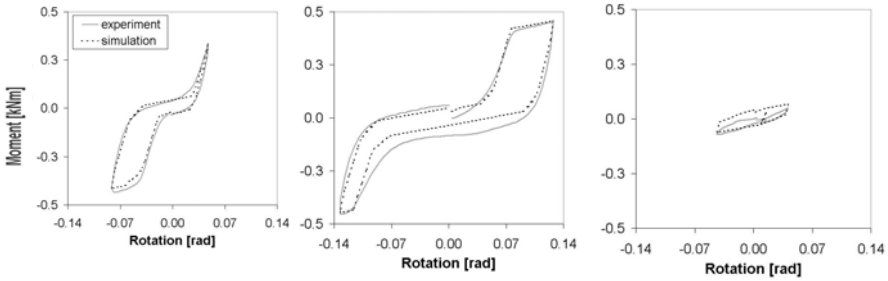

Cycle no. 16 **Cycle no. 30** **Cycle no. 46**

Figure 15. Simulation versus experimental results for selected cycles

An examination of the predicted response for the selected cycles shows good agreement with the experiments. Some deficiencies are apparent such as more predicted pinching (Figure 15 cycle no.30) and incorrectly predicting the degradation in cycle no. 46 with small amplitude. However, the developed hysteretic model sufficiently

reproduces the cyclic behavior of the connection well into the plastic range.

Having demonstrated the effectiveness of the model to simulate the load-deformation path, examination of the area enclosed by the hysteretic loops will further demonstrate the ability to estimate the energy dissipation capacity. The energy dissipation per cycle and the cumulative dissipation are plotted versus the cycle number in Figure 16a and b, respectively.

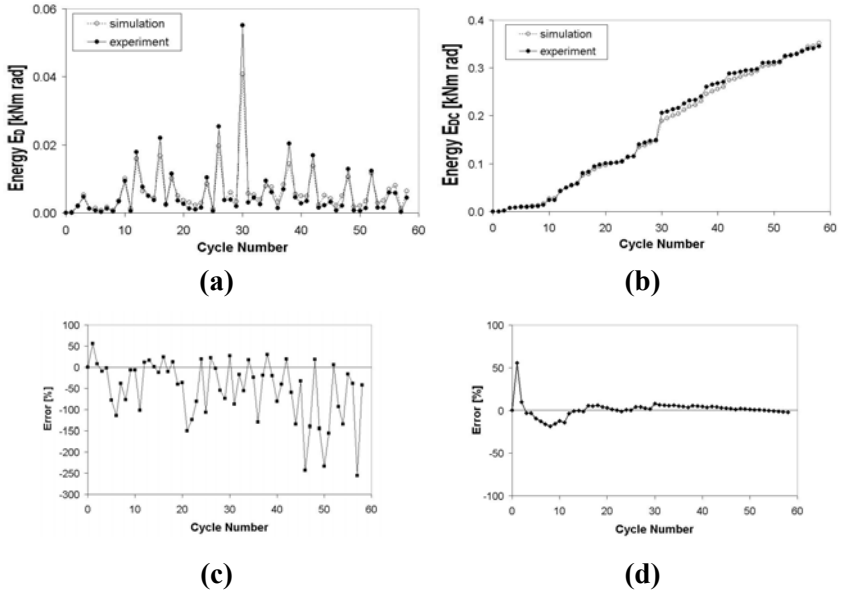

Figure 16. Simulation versus experimental results for (a) energy dissipated per cycle, (b) cumulative energy dissipated, (c) error in energy dissipated per cycle and (d) error in cumulative energy dissipated

Comparison of analytical and experimental results show that the energy dissipation was estimated reasonably well with the cumulative energy prediction more accurate than the per cycle prediction. From Figure 16a generally the model underestimated the energy dissipation capacity for large-amplitude cycles ($\varphi > 0.04$ rad) and overestimated the capacity for low-amplitude cycles ($\varphi < 0.04$ rad). Therefore, the

error in cumulative energy (Figure 16d) is small, since the deficits of large-amplitude cycles were equalized by low-amplitudes. An examination of the error per cycle shows that the differences in energy dissipation can be quite large (Figure 16c). The cycles with large errors are low-amplitude cycles (such as cycle no. 46) whereby the error increases as the test progresses. The reason for the increase in error is that the model represents simplified behavior and does not capture the interaction between the deformation in wood and the steel dowels. For instance, a steel dowel in an oversized hole is sliding and will not carry any load until it is in contact with the wood again. Such slippage significantly influences the hysteresis of low-amplitude cycles. However, small cycles are of minor importance for the total energy dissipated in the system. Thus the model is accurate in modeling the response of the connection to an arbitrary load but the precision is poor for low amplitudes.

4 CONCLUSIONS

Local reinforcement of timber structural components can effectively control brittle failure modes and prevent crack development and/or propagation. Initial laboratory and full-scale experiments demonstrated the feasibility of such approaches. In order for these methods to gain applicability in design, a number of issues need to be studied. These include the effect of differential shrinkage, swelling and thermo expansion on interface and stresses, the effect of long-term loading (creep, mechano-sorptive creep and the effect of cyclic loading combined with an environmental load), and the effect of aggressive environment and elevated temperatures (short- and long term including fire). Short-term laboratory experiments showed the effectiveness of local reinforcement but application in structures will require addressing the above issues.

5 ACKNOWLEDGMENT

The help of Dr.-Ing. Andreas Heiduschke, TU Dresden, with experiments and data analysis and Mr. William Brian, North Carolina State University, with specimen preparation is gratefully acknowledged. This paper is based on author's published original work listed in cited literature.

6 LITERATURE CITED

1. Kasal, B., and A. Heiduschke. 2004. Radial reinforcement of glue laminated wood beams with composite materials. Forest Product Journal. 54 (1): 74-79
2. Goetz, K.H., D. Hoor, K. Moehler, and J. Natterer. 1989. Timber design & construction sourcebook. McGraw-Hill Publishing Company. New York. NY. 288 p.
3. National Design Specification for Wood Construction (NDS) ASD/LRFD. 2005. ANSI/ AF&PA. Washington D.C. ISBN 0-9625985-1-8
4. Timber Engineering STEP 1. Centrum Hout. The Netherlands. 1995.
5. DIN 1052:2004-08 "Entwurf, Berechnung und Bemessung von Holzbauwerken - Allgemeine Bemessungsregeln und Bemessungsregeln für den Hochbau".
6. Kasal, B., Heiduschke, A., Kadla, J. and Haller, P. 2004. Laminated timber frames with composite fiber reinforced connections. Progress in Structural Engineering and Materials, John Wiley & Sons Ltd. London, UK, Vol. 6, Issue 2: 84-93.
7. Haller, P. and Chen, C. J. 1999. Textile reinforced timber joints and structures. Structural Engineering International, 4/99: 259-261.
8. Haller, P. and Wehsener, J. 2003. Entwicklung innovativer Verbindungen aus Pressholz und Glasfaserarmierungen für den Ingenieurholzbau. Frauenhofer IRB-Verlag, Stuttgart, T3003.
9. Wehsener, J., and B. Kasal. 2008. Echtzeit-Röntgenuntersuchungen and duktilen stabförmigen Holzverbindungen bei dynamischer Beanspruchung. Bautechnik 85 (2008), Heft 10. Ernst & Sohn Verlag für Architektur und technische Wissenschaften GmbH & Co. KG, Berlin: 678-686.
10. Sozen, M. Hysteresis in structural elements. Applied Mechanics and Earthquake Engineering, Iwan WD (ed.), ASME: New York, pp. 63-98, 1974.
11. DIN EN 12512. Timber Structures – Test methods – Cyclic testing of joints made with mechanical fasteners. German Version EN 12512:2001, Beuth Verlag, Berlin, Germany, 2002.
12. ANSYS MANUAL Release 8.0 – ANSYS Inc., Canonsburg, PA, USA.

13. Petersen, C. Dynamik der Baukonstruktionen. Vieweg & Sohn Verlagsgesellschaft, Braunschweig/Wiesbaden, Germany, 1996.
14. Ceccotti, A. and Vignoli, A. A pinching model for semi-rigid joints. European earthquake Engineering Journal, Bologna Itally, Vol. 3, pp. 3-9, 1993.
15. Foliente, G. C. Hysteresis modeling of wood joints and structural systems. Journal of Structural Engineering, 121(6), 1013-1022, 1995.
16. Richard, N., Yasumura, M. and Davenne, L. Prediction of seismic behavior of wood-framed shear walls with openings by pseudodynamic tests and FE-model. Journal of wood Science Vol.49 pp. 145-151, 2003.
17. Powel, G. H. DRAIN-2DX User guide. Dept. of Civil Eng., University of California, Berkeley, 1993.
18. Kasal, B., and , H. Xu. 1997. A mathematical model of connections with nonlinear nonconservative hysteretic behavior. In Earthquake performance and safety of timber structures. FPS proceedings No. 7289. FPS, Madison, WI. 105-107.
19. Kasal, B., and H. Xu. 1996. A nonlinear nonconservative finite-element with hysteretic behavior and memory. 7th International ANSYS Conference. Philadelphia, PA. 3. 235-3.242.
20. Collins, M. Kasal, B., Paevere, P. and Foliente, G. C. Three-dimensional model of light frame wood buildings. I: Model formulation. Journal of Structural Engineering, ASCE, 131(4), 676-683, 2005.
21. Foliente, G. C., Paevere, P. and Ma, F. Parameter Identification and Seismic Response Analysis of Timber Structures. Proceedings of WCTE Montreux, Switzerland, Vol.2. 532-539, 1998.
22. Fajfar, P. and Drobnic, D. Non-linear seismic analysis of a semi-rigid frame building. In: IABSE Colloquium. Istanbul, Editor: ETH-Hoenggerberg, Zuerich, Switzerland, 1996.
23. Pradhan, A. M. Experimental and numerical studies on earthquake response of composite beam-column connections. Technical University Darmstadt - Dissertation, 1998.
24. Kawai, N. Seismic performance testing on Wood Framed Shear Wall. Proceedings CIB-W18-meeting, Savonlinna, Finland, Universität Karlsruhe CIB W18/31-15-1, 1998.

25. DIN EN 12512. Timber Structures – Test methods – Cyclic testing of joints made with mechanical fasteners. German Version EN 12512:2001, Beuth Verlag, Berlin, Germany, 2002.
26. Kasal, B., Pospíšil, S., Jirovsy, I., Heiduschke, A., Drdacky, M. and Haller, P. Seismic performance of laminated timber frames with fiber reinforced connections. Earthquake Engineering and Structural Dynamics. John Wiley & Sons Ltd. London, UK, Vol. 33. (5): 633-646, 2004.

CURRICULUM VITAE

Professional Preparation

Institution	Major	Minor	Degree	Year
TU Zvolen	Wood Technology	-	Ing.; Summa Cum Laude	1980
Virginia Polytechnic Institute and State University	Wood Composites	-	MS	1989
Oregon State University, Corvallis, Oregon	Civil Engineering	-	MS	1993
Oregon State University, Corvallis, Oregon	Wood Mechanics	Mathematics and Structural Engineering	PhD	1992

Appointments

Dates	Appointment	Institution
2005-present	Hankin Chair Professor of Civil and Environmental Engineering Professor of Architectural Engineering	Department of Civil and Environmental Engineering, Pennsylvania State University, State College, PA
2005-present	Director, Pennsylvania Housing Research Center	Pennsylvania State University, State College, PA
2003-2005	Professor	Department of Wood and Paper Science, North Carolina State University, Raleigh, NC
2001-2002	Visiting Professor and Senior Fulbright Fellow	Department of Civil Engineering, TU Dresden, Germany
1994-2003	Associate Professor	Department of Wood and Paper Science, North Carolina State University, Raleigh, NC
1994-2005	Associate Professor, Professor (Associate Faculty)	Department of Civil Engineering, North Carolina State University, Raleigh, NC

1992-1994	Assistant Professor	Department of Wood and Paper Science, North Carolina State University, Raleigh, NC
1992	Research and Development Engineer	ALPINE Engineered Products, Inc., Pompano Beach, FL

Teaching
Residential design and construction; Wood mechanics; Advanced wood design; Historic construction techniques; Wood composites; Sustainable urban design; Building envelope science and design

Synergistic Activities
1. Headed international research team from four countries to study application of high-strength composite materials in dynamically loaded timber structures.
2. Awarded 2001/2002 Fulbright Scholarship to Germany. Invited as International Fulbright Lecturer to France, Sweden, Czech Republic and institutions in Germany. Lectured in Japan, Chile, Switzerland, Finland, Australia, Austria, Germany, Great Britain, Sweden, Hungary, Slovakia, Czech Republic. Invited research presentation to 50th Anniversary of Fulbright Program attended by the President of Germany, US Ambassador to Germany, German Foreign Minister and other officials.
3. Chair, RILEM TC on In-situ evaluation of timber structures. Editorial Advisory Committee of Journal of Materials and Structures.
4. Developed, as one of the 1st, a model for analysis of light-frame structural systems. Conducted unique full scale, full-instrumented experiments on light-framed structures.
5. Developed web-based courses in Structural Design in Wood, Mechanics of Wood Composites and Wood Mechanics. Awarded NSF REU grants to involve undergraduate students in research. Developed a course Introduction to historic construction techniques; Advanced wood design;

Membership in Professional Organizations
American Academy of Mechanics, American Society of Experimental Mechanics, Society for Earthquake and Engineering Dynamics, International Conference of Building Officials, American Society of Civil Engineers, Structural Engineering Institute of the ASCE, National Geographic Society, RILEM;US Congress Caucus for Wind Hazard in Housing, FEMA Disaster Inspector.

Publications
Over 100 publications.